

## Antiferrodistortive phase transition in $\text{Pb}(\text{Ti}_{0.48}\text{Zr}_{0.52})\text{O}_3$ : A powder neutron diffraction study

Rajeev Ranjan, Ragini, S. K. Mishra, and Dhananjai Pandey

*School of Materials Science and Technology, Institute of Technology, Banaras Hindu University, Varanasi-221005, India*

Brendan J. Kennedy

*School of Chemistry, The University of Sydney, Sydney, NSW 2006, Australia*

(Received 29 August 2001; published 24 January 2002)

Results of a powder neutron diffraction study of the high-temperature monoclinic ( $F_M^{\text{HT}}$ ) to a low-temperature monoclinic ( $F_M^{\text{LT}}$ ) phase transition in  $\text{Pb}(\text{Ti}_{1-x}\text{Zr}_x)\text{O}_3$  discovered recently by Ragini *et al.* are presented for  $x=0.520$ . The powder neutron diffraction pattern of the  $F_M^{\text{LT}}$  phase contains superlattice reflections which have all odd  $hkl$  ( $h \neq k \neq l$ ) Miller indices with respect to a doubled elementary perovskite cell, characteristic of antiphase tilting of oxygen octahedra. In analogy to other perovskite systems, the appearance of these superlattice reflections is attributed to an instability at the R point of the cubic Brillouin zone. We show that the most plausible space group of the  $F_M^{\text{LT}}$  phase is Pc. Results of Rietveld refinement for this space group are presented to show that the oxygen octahedra indeed undergo antiphase rotations about [001] direction.

DOI: 10.1103/PhysRevB.65.060102

PACS number(s): 77.84.Dy, 81.30.Hd, 61.12.Ld

The solid solution  $\text{Pb}(\text{Ti}_{1-x}\text{Zr}_x)\text{O}_3$  (PZT) system is a well known piezoelectric ceramic material with immense technological applications.<sup>1</sup> The phase diagram of this system shows a nearly vertical morphotropic phase boundary (MPB) around  $x=0.52$  (Ref. 1) separating the ferroelectric tetragonal ( $F_T$ ) and the ferroelectric rhombohedral ( $F_R$ ) phase regions. The most precise location of the MPB was made by Mishra *et al.*,<sup>2,3</sup> who showed that the room-temperature structure of PZT is tetragonal and rhombohedral for  $x \leq 0.520$  and  $x \geq 0.530$ , respectively, while both the phases coexist for  $x=0.525$  at 300 K.<sup>1</sup> Very interesting aspects of the phase transition behavior of PZT ceramics near the MPB composition were also reported by Mishra *et al.*<sup>2-4</sup> using high-temperature x-ray diffraction (XRD), piezoelectric resonance frequency ( $f_r$ ), electromechanical coupling coefficient ( $k_p$ ), and dielectric constant ( $\epsilon'$ ) measurements in the temperature range 300–800 K. These workers have shown that the  $F_T$  (space group  $P4mm$ ) to the paraelectric cubic (space group  $Pm3m$ ) phase transition is of first order in the composition range  $0.515 \leq x < 0.550$  ( $T_C=676, 667, 662,$  and  $651$  K for  $x=0.0515, 0.520, 0.530,$  and  $0.535$  during heating) while the  $F_R$  (space group  $R3m$ ) to  $P_C$  direct transition ( $T_C=634$  K for  $x=0.550$ ) for  $x \geq 0.550$  is of second order type implying thereby the possibility of a tricritical point for  $0.545 < x < 0.550$ .<sup>4</sup> For  $x=0.525$ , the coexistence of the  $F_T$  and  $F_R$  phases at 300 K was shown to be linked with the  $F_R$  to  $F_T$  first-order phase transition. The  $F_R$  to  $F_T$  transition for  $0.530 \leq x < 0.550$  was also found to be accompanied with a coexistence region.

Recently, Noheda *et al.*<sup>5,7</sup> carried out a very careful high-resolution synchrotron study of low-temperature phase transitions in PZT and showed that the  $F_T$  phase for  $x=0.500, 0.520$  transforms at 200 K and 250 K into a ferroelectric monoclinic ( $F_M^{\text{HT}}$ ) phase with space group Cm. Phenomenological theory considerations of Filho *et al.*<sup>8</sup> and Vanderbilt and Cohen<sup>9</sup> have confirmed the stability of a monoclinic phase. Ragini *et al.*,<sup>10</sup> on the other hand, found

evidence for two low-temperature phase transitions for  $x=0.515$  and  $0.520$  in their piezoelectric resonance frequency ( $f_r$ ) and dielectric ( $\epsilon'$ ) studies. Correlating the two anomalies in  $f_r(T)$  and  $\epsilon'(T)$  data with XRD and electron diffraction data, Ragini *et al.*<sup>10</sup> have confirmed that the first anomaly occurring just below room temperature is due to the  $F_T$  to  $F_M^{\text{HT}}$  transition studied by Noheda *et al.*<sup>5,6</sup> The second anomaly in  $\epsilon'(T)$  and  $f_r(T)$ , discovered by Ragini *et al.*<sup>10</sup> is due to a phase transition from  $F_M^{\text{HT}}$  to another monoclinic ( $F_M^{\text{LT}}$ ) phase whose  $a$  and  $b$  parameters are identical to the  $F_M^{\text{HT}}$  phase but the  $c$  parameter is doubled. It was shown by Ragini *et al.*<sup>10</sup> that the  $F_M^{\text{HT}}$  to  $F_M^{\text{LT}}$  phase transition gives rise to superlattice reflections in the electron diffraction patterns which are not discernible on the XRD patterns as a result of which Noheda *et al.*<sup>5,6</sup> missed this transition in their synchrotron XRD studies.

Using first principle calculations, Bellaiche *et al.*<sup>11</sup> have shown that even at room temperature, the  $F_T$  and  $F_R$  phase regions across the MPB are separated by a narrow composition range over which the  $F_M^{\text{HT}}$  phase is more stable than the  $F_T$  or  $F_R$  phases. Ragini *et al.*<sup>12</sup> have carried out a detailed Rietveld study of the room temperature structure of PZT phases across the MPB and have come to the conclusion that the stable phase of PZT at 300 K for  $0.525 \leq x < 0.70$  is not rhombohedral but monoclinic. Further, the  $F_T$  to  $F_M^{\text{HT}}$  to  $F_M^{\text{LT}}$  sequence of phase transitions, discovered by Ragini *et al.*<sup>10</sup> for  $x=0.515$  and  $0.520$ , is a common feature of all the PZT compositions in the range  $0.515 \leq x < 0.550$ .<sup>13</sup>

While the low and high temperature phase transition aspects of PZT ceramics in the MPB region are now reasonably well settled, the structure of the  $F_M^{\text{LT}}$  phase remains unknown. Noheda *et al.*<sup>5,6</sup> have proposed Cm space group for the low temperature monoclinic phase of PZT with  $x=0.520$  using a Rietveld analysis of the synchrotron data at 20 K. Since 20 K for  $x=0.520$  is well below the  $F_M^{\text{HT}}$  to  $F_M^{\text{LT}}$  phase transition temperature of 210 K, Ragini *et al.*<sup>10</sup> have

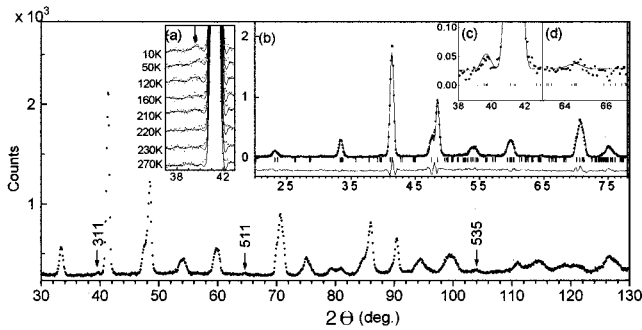


FIG. 1. Powder neutron diffraction pattern of  $\text{Pb}(\text{Ti}_{0.48}\text{Zr}_{0.52})\text{O}_3$  at 10 K. The three arrows indicate superlattice reflections. The Miller indices are with respect to a doubled elementary perovskite cell ( $2a_p \times 2b_p \times 2c_p$ ). Inset (a) depicts evolution of superlattice reflection 311 as a function of temperature. Inset (b) shows observed (dots), calculated and difference profiles (continuous line) in the two-theta range 20–80 degree after Rietveld refinement with  $Pc$  space group. Insets (c) and (d) depict fit of two of the superlattice reflections after the refinement.

questioned the correctness of this space group at 20 K since it cannot account for the observed superlattice reflections in the electron diffraction patterns. The purpose of this communication is to present powder neutron diffraction data for  $x = 0.520$  in the temperature range 280 K to 10 K to show that weak superlattice reflections appear below the  $F_M^{\text{HT}}$  to  $F_M^{\text{LT}}$  phase transition temperature of 210 K. It is shown that these superlattice reflections have all odd  $hkl$  ( $h \neq k \neq l$ ) Miller indices. In analogy to other perovskite materials,<sup>14</sup> the appearance of such superlattice reflections is attributed to an AFD phase transition involving oxygen octahedral tilts driven by instabilities at the  $R$ -point ( $q = \frac{1}{2}, \frac{1}{2}, \frac{1}{2}$ ) of the Brillouin zone. Further, we propose a structural model for the  $F_M^{\text{LT}}$  phase with space group  $Pc$  and refine the structure of the  $F_M^{\text{LT}}$  phase using Rietveld technique.

Highly homogeneous and strictly stoichiometric PZT samples were prepared by a novel semi-wet route the details of which are described elsewhere.<sup>15</sup> Powder neutron diffraction data were recorded in the  $2\theta$  range of 20 to 130 degrees at a step of 0.10 degree using neutron wavelength of 1.667 Å on a medium resolution powder diffractometer on High Flux Australian Reactor (HIFAR) operated by the Australian Nuclear Science and Technology Organization (ANSTO). The powdered sample was compacted in a thin walled 12 mm diameter vanadium cylinder and then placed inside a displax cryostat. The powder neutron diffraction data were collected at various temperatures between 10 K to 280 K while heating. The temperature was controlled within  $\pm 2$  K. Structure refinement was performed using Rietveld refinement program DBWS 9411.<sup>16</sup> The background was defined by a sixth order polynomial in two-theta. A pseudo-Voigt function was chosen to generate profile shape for the neutron diffraction peaks.

Figure 1 depicts the powder neutron diffraction pattern of PZT with  $x = 0.52$  at 10 K. All the peaks, except those marked with arrows, in this figure can be indexed with respect to a monoclinic cell of the type proposed by Noheda *et al.*<sup>5,6</sup> with  $a = 5.730$  Å,  $b = 5.709$  Å and  $c = 4.117$  Å,  $\beta$

$= 90.48^\circ$ . The three weak reflections, marked with arrows in Fig. 1, appear at  $T \leq 210$  K as can be seen from the inset (a) which depicts the temperature evolution of one of these weak reflections. This temperature ( $\sim 210$  K) coincides with the  $F_M^{\text{HT}}$  to  $F_M^{\text{LT}}$  phase transition temperature of PZT with  $x = 0.52$  reported by Ragini *et al.*<sup>10</sup> Indexing of all the reflections in Fig. 1, including the weak ones, requires a monoclinic cell whose  $c$ -parameter is twice that of the  $F_M^{\text{HT}}$  phase. The weak reflections are thus superlattice reflections linked with a cell doubling transition.

Superlattice reflections in the  $\text{ABO}_3$  perovskites can result from antiferrodistortive (AFD) structural phase transitions. The most common AFD transitions in perovskites involve octahedral tilts (rotations) brought about by instabilities at the  $R$  ( $q = \frac{1}{2}, \frac{1}{2}, \frac{1}{2}$ ) and  $M$  ( $q = \frac{1}{2}, \frac{1}{2}, 0$ ) points of the cubic Brillouin zone. The familiar examples are structural phase transitions in  $\text{SrTiO}_3$ ,<sup>14</sup>  $\text{LaAlO}_3$ <sup>17</sup> and  $\text{KMnF}_3$ .<sup>18</sup> With respect to a pseudocubic cell of the type  $2a_p \times 2b_p \times 2c_p$ , where  $a_p$ ,  $b_p$ , and  $c_p$  are the unit cell parameters of the elementary perovskite cell, the main perovskite reflections are represented by Miller indices which are all even ( $e$ ) numbers (i.e., the Miller indices are of  $eee$  type). The superlattice reflections arising due to AFD phase transitions correspond to three or two odd ( $o$ ) numbered Miller indices which arise due to cell doubling along all the three or at least two of the elementary perovskite  $\langle 100 \rangle$  directions.<sup>19</sup> As was shown by Glazer,<sup>19</sup> superlattice reflections with all-odd ( $ooo$ ) ( $hkl, h \neq k \neq l$ ) Miller indices arise due to “anti-phase” (or  $-ve$ ) tilt of the neighboring octahedra whereas superlattice reflections with two-odd and one-even ( $ooe$ ) type Miller indices are due to “in-phase” (or  $+ve$ ) tilt. These “+” and “−” tilts are believed to result from the freezing of the soft modes of the  $M$  and  $R$  points of the cubic Brillouin zone as confirmed in materials like  $\text{KMnF}_3$ ,<sup>18</sup>  $\text{CsPbCl}_3$ ,<sup>20</sup> and  $\text{SrTiO}_3$ <sup>14</sup> using inelastic neutron scattering. With respect to the doubled perovskite cell, the superlattice reflections in Fig. 1 assume 311, 511, and 535 Miller indices which are of “ $ooo$ ” type. This implies that these reflections have arisen due to antiphase (−) tilting of  $\text{TiO}_6$  octahedra in the neighboring elementary perovskite cell. Thus the  $F_M^{\text{HT}}$  to  $F_M^{\text{LT}}$  phase transition discovered by Ragini *et al.*<sup>10</sup> is an AFD phase transition involving  $R$ -point instability.

As said earlier, Noheda *et al.*<sup>5,6</sup> have refined the structure of the low temperature phase of PZT with  $x = 0.52$  using the  $Cm$  space group, but this space group cannot give rise to the superlattice reflections present in Fig. 1. In the Glazer’s classification<sup>19</sup> of perovskite structures with tilted oxygen octahedra, there are only three monoclinic space groups,  $P2_1/m$ ,  $C2/m$  and  $C2/c$  corresponding to  $a^+b^-c^-$ ,  $a^0b^-c^-$  and  $a^-b^-b^-$  tilt systems. Of these, the  $a^+b^-c^-$  tilt system is ruled out since the superlattice reflections observed in Fig. 1 are of “ $ooo$ ” type only. The remaining two tilt systems are although compatible with the “ $ooo$ ” type superlattice reflections, their space groups are centrosymmetric. Since the  $F_M^{\text{LT}}$  phase is a ferroelectric phase, it rules out any centrosymmetric space group. Thus none of the space groups listed by Glazer<sup>19</sup> can describe the structure of the  $F_M^{\text{LT}}$  phase.

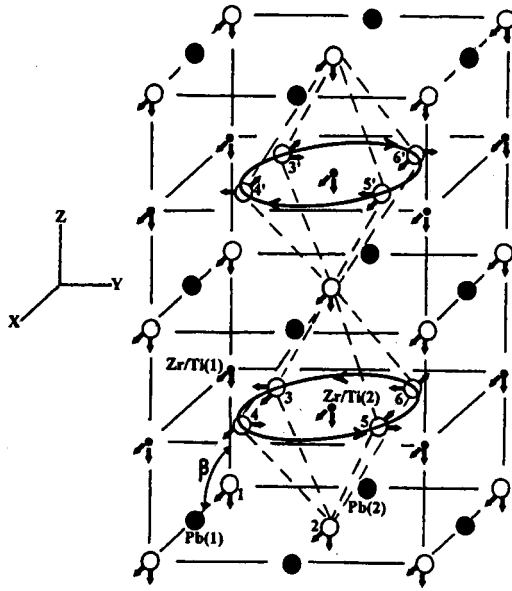


FIG. 2. Schematic diagram of the doubled monoclinic unit cell showing superposition of antiphase rotation of octahedra (about [001] direction) and other atoms, i.e., O(1), O(2), Pb(1), Pb(2), Zr/Ti(1), and Zr/Ti(2), displaced as in the  $Cm$  space group model. The open circles, filled big circles and the filled small circles represent O, Pb, and Zr/Ti, respectively. The arrows indicate sense of displacements from their respective undisplaced positions.

Rietveld analysis of the powder neutron diffraction data given in Fig. 1 using  $Cm$  space group accounts reasonably well for all the peaks except the superlattice ones. In view of this, the structure of the  $F_M^{LT}$  phase should not only retain the main structural features of the  $Cm$  space group model but also account for the weak superlattice reflections present in Fig. 1. For this, we propose here a new structural model. Consider the stacking of two monoclinic unit cells of the  $Cm$  type in the [001] direction as shown in Fig. 2. On superposing  $a^0a^0c^-$  tilt on this structural model, the four oxygen atoms labeled as 3, 4, 5 and 6 in the  $z = \frac{1}{4}$  plane will rotate in anticlockwise and another set of four oxygen atoms labeled as 3', 4', 5' and 6' in the  $z = \frac{3}{4}$  plane in the clockwise manner about [001] by equal magnitude. As a result of such an anti-phase tilt about the [001] direction, the  $C$ -centring and the mirror plane at  $y=0, \frac{1}{2}$  of the  $Cm$  space group are destroyed. The doubled monoclinic unit cell is now a primitive cell with  $c$ -glide planes at  $y=0, 1/2$ . It is easy to see that the pair of atoms 3-6', 4-5', 5-4', and 6-3' in the  $z = \frac{1}{4}$  and  $\frac{3}{4}$  layers are related through a  $c$ -glide at  $y = \frac{1}{2}$ . There are only four non-centrosymmetric monoclinic space groups viz.,  $P2$ ,  $P2_1$ ,  $Pm$  and  $Pc$ .<sup>21</sup> Of these, only  $Pc$  has got a  $c$ -glide plane consistent with the model proposed by us, and was accordingly chosen for refining the structure of the  $F_M^{LT}$  phase.

The  $Pc$  space group possesses only one site symmetry ( $2a$  Wyckoff position) having general coordinates. Therefore, in principle all the coordinates can be refined independently. The asymmetric unit of the structure consists of two Pb atoms, two Zr/Ti atoms and six O atoms. Fixing one atom at

the origin, the total number of refinable positional coordinates and isotropic thermal parameters, in principle, comes out to be 37. But in keeping with the  $Cm$  framework, which accounts for the intensity of all the main perovskite peaks, the positions of both the Pb atoms in the asymmetric unit were not refined. Similarly Zr/Ti(1), Zr/Ti(2) atoms and the O(1) and O(2) atoms in the asymmetric unit were treated as identical, and their sense of displacements from their respective undisplaced coordinates were kept identical to those given by Noheda *et al.*<sup>6</sup> for the  $Cm$  space group. These displacements contribute to the intensity of the main perovskite reflections only and not to the weak superlattice reflections in Fig. 1. As a result of an anticlockwise rotation of the lower oxygen octahedra in Fig. 2 about the [001] direction, the  $x, y$  coordinates of the four oxygen atoms 3, 4, 5, and 6 will become  $(0.25 + \delta, 0.25 - \delta)$ ,  $(0.75 + \delta, 0.25 + \delta)$ ,  $(0.75 - \delta, 0.75 + \delta)$ , and  $(0.25 - \delta, 0.75 - \delta)$  where  $\delta$  is the parameter to be refined for determining the magnitude of the fractional displacements. In this model, there are six independently refinable positional coordinates and four isotropic thermal parameters. Refinement of these parameters along with the half width, background, zero correction, and lattice parameters led to smooth convergence of the  $R$ -factors within a few cycles with a satisfactory  $\chi^2 (=1.59)$  value. Table I lists the various structural parameters along with the  $R$  factors obtained at the end of the refinement. The observed, calculated and the difference profiles shown in inset (b) of Fig. 1 indicate a reasonable fit for various reflections including the weak superlattice reflections which is shown insets (c) and (d) of Fig. 1 on a magnified scale. After having got a satisfactory  $\chi^2$  value, we allowed fractional displacement parameter ( $\delta$ ) to be different for the  $x$  and  $y$  coordinates of the 3, 4, 5 and 6 oxygen atoms of the asymmetric unit. As a result, the number of refinable parameters is now one more than that in the earlier model. Such a relaxation in  $\delta$  led to a decrease in  $R_{wp}$  from 8.95 (obtained for model I with only one  $\delta$  parameter) to 8.84 (obtained for model II with two ' $\delta$ 's). The various refined structural parameters along with the  $R$  factors for model II are given in Table I along with those for model I.

A comparison of the refined structural parameters for model II with those reported by Noheda *et al.*<sup>5,6</sup> reveals that, except for the  $y$ -coordinates of the planar oxygen atoms (3, 4, 5 and 6 in Fig. 2), rest of the refined coordinates in model II are almost identical to those for the  $Cm$  space group model. On the other hand, for model I, all the three coordinates of the four oxygen atoms (3, 4, 5 and 6) are quite different from those for the  $Cm$  model even though the coordinates of the other atoms are in good agreement for the two models. It is however, difficult to make a choice between models I and II using the present data since the reduction in the agreement factor ( $R_{wp}$ ) for model II is not very significant.

To summarize, we have observed superlattice reflections in powder neutron diffraction data below the  $F_M^{HT}$  to  $F_M^{LT}$  phase transition temperature of  $\sim 210$  K in PZT with  $x = 0.520$ . These superlattice reflection are attributed to an antiferrodistortive (AFD) phase transition involving antiphase tilts of the oxygen octahedra. In analogy to other perovskites



TABLE I. Refined structural parameters and  $R$  factors of PZT with  $x=0.52$ . In model I, the  $x$  and  $y$  coordinates of O(3), O(4), O(5), and O(6) were refined with one common fractional displacement ( $\delta$ ) parameter. In model II the  $x$  and  $y$  coordinates of these atoms were refined with different  $\delta$  parameters.

Atom	Model I				Model II			
	$x$	$y$	$z$	$B$ ( $\text{\AA}^2$ )	$x$	$y$	$z$	$B$ ( $\text{\AA}^2$ )
Pb(1)	0.50	0.00	0.00	2.8(2)	0.50	0.00	0.00	1.4(2)
Pb(2)	0.00	0.50	0.00	2.8(2)	0.00	0.50	0.00	1.4(2)
Zr/Ti(1)	0.013(6)	0.00	0.225(2)	0.4(3)	0.028(6)	0.00	0.222(2)	0.3(3)
Zr/Ti(2)	0.513(6)	0.50	0.225(2)	0.4(3)	0.528(6)	0.50	0.222(2)	0.3(3)
O(1)	0.056(2)	0.00	-0.045(1)	0.1(2)	0.051(2)	0.00	-0.044(1)	1.2(2)
O(2)	0.556(2)	0.50	-0.045(1)	0.1(2)	0.551(2)	0.50	-0.044(1)	1.2(2)
O(3)	0.261(1)	0.239(1)	0.267(1)	0.3(1)	0.289(8)	0.235(1)	0.195(1)	0.4(2)
O(4)	0.761(1)	0.261(1)	0.267(1)	0.3(1)	0.789(8)	0.265(1)	0.195(1)	0.4(2)
O(5)	0.739(1)	0.761(1)	0.267(1)	0.3(1)	0.791(8)	0.765(1)	0.195(1)	0.4(2)
O(6)	0.239(1)	0.739(1)	0.267(1)	0.3(1)	0.291(8)	0.735(1)	0.195(1)	0.4(2)

$a=5.731(1)$   $\text{\AA}$ ,  $b=5.710(1)$   $\text{\AA}$ ,  $c=8.234(1)$   $\text{\AA}$   
 $\beta=90.49(1)^\circ$   
 $R_B=6.01$ ,  $R_p=7.10$ ,  $R_{wp}=8.95$ ,  $R_e=8.09$

$a=5.732(1)$   $\text{\AA}$ ,  $b=5.708(1)$   $\text{\AA}$ ,  $c=8.235(1)$   $\text{\AA}$   
 $\beta=90.49(1)^\circ$   
 $R_B=4.23$ ,  $R_p=6.95$ ,  $R_{wp}=8.84$ ,  $R_e=8.08$

like SrTiO<sub>3</sub>, we propose that this transition is driven by instabilities at the  $R$ -point ( $q=\frac{1}{2}\frac{1}{2}\frac{1}{2}$ ) of the cubic Brillouin zone. The  $Cm$  space group proposed by Noheda *et al.*<sup>6</sup> for the monoclinic phase of PZT with  $x=0.520$  at 20 K cannot account for the observed superlattice reflections. We have shown that the correct space group of the  $F_M^{LT}$  phase is  $Pc$ . The positional coordinates of some of the atoms obtained by Rietveld refinement using  $Pc$  space group bear close resemblance

with those obtained by Noheda *et al.* using  $Cm$  space group.

Partial support from Inter University Consortium for the Department of Atomic Energy Facilities is gratefully acknowledged by the authors from BHU. S.K.M. is grateful to CSIR for financial support. B.K.J. thanks the Australian Institute of Nuclear Science and Engineering for the provision of the neutron scattering facilities.

- <sup>1</sup>B. Jaffe, W. R. Cook, and H. Jaffe, *Piezoelectric Ceramics* (Academic Press, London/New York, 1971).
- <sup>2</sup>S. K. Mishra, A. P. Singh, and D. Pandey, *Appl. Phys. Lett.* **69**, 1707 (1996).
- <sup>3</sup>S. K. Mishra, A. P. Singh, and D. Pandey, *Philos. Mag. B* **76**, 213 (1997).
- <sup>4</sup>S. K. Mishra and D. Pandey, *Philos. Mag. B* **76**, 227 (1997).
- <sup>5</sup>B. Noheda, D. E. Cox, G. Shirane, J. A. Gonzalo, L. E. Cross, and S. E. Park, *Appl. Phys. Lett.* **74**, 2059 (1999).
- <sup>6</sup>B. Noheda, J. A. Gonzalo, L. E. Cross, R. Guo, S. E. Park, D. E. Cox, and G. Shirane, *Phys. Rev. B* **61**, 8687 (2000).
- <sup>7</sup>B. Noheda, D. E. Cox, G. Shirane, R. Guo, B. Jones, and L. E. Cross, *Phys. Rev. B* **63**, 014103 (2000).
- <sup>8</sup>A. G. Souza Filho, K. C. V. Lima, A. P. Ayala, I. Guedes, P. T. C. Freire, J. Mendes Filho, E. B. Arauzo, and J. A. Eiras, *Phys. Rev. B* **61**, 14 283 (2000).
- <sup>9</sup>D. Vanderbilt and M. H. Cohen, *Phys. Rev. B* **63**, 094108 (2001).
- <sup>10</sup>Ragini, S. K. Mishra, D. Pandey, H. Lemmens, and G. Van Tendeloo, *Phys. Rev. B* **64**, 054101 (2001).
- <sup>11</sup>L. Bellaiche, A. Garcia, and D. Vanderbilt, *Phys. Rev. Lett.* **84**, 5427 (2000).
- <sup>12</sup>Ragini, Rajeev Ranjan, S. K. Mishra, and D. Pandey (unpublished).
- <sup>13</sup>Ragini, Rajeev Ranjan, S. K. Mishra, and D. Pandey (unpublished).
- <sup>14</sup>A. D. Bruce and R. W. Cowley, *Adv. Phys.* **29**, 219 (1980).
- <sup>15</sup>A. P. Singh, S. K. Mishra, D. Pandey, Ch. D. Prasad, and R. Lal, *J. Mater. Sci.* **28**, 5050 (1993).
- <sup>16</sup>R. A. Young, A. Sakthivel, T. S. Moss, and C. Paiva Santos, Program DBWS-9411 for Rietveld analysis for X-ray and Neutron Powder Diffraction Patterns, 1994.
- <sup>17</sup>C. J. Howard, B. J. Kennedy, and B. C. Chakoumakos, *J. Phys.: Condens. Matter* **12**, 349 (2000).
- <sup>18</sup>V. J. Minkiewicz and G. Shirane, *J. Phys. Soc. Jpn.* **26**, 674 (1969).
- <sup>19</sup>A. M. Glazer, *Acta Crystallogr., Sect. B: Struct. Crystallogr. Cryst. Chem.* **B28**, 3384 (1972); *Acta Crystallogr., Sect. A: Cryst. Phys., Diffir., Theor. Gen. Crystallogr.* **A31**, 756 (1975).
- <sup>20</sup>Y. Fuji, S. Hoshino, Y. Yamada, and G. Shirane, *Phys. Rev. B* **10**, 4549 (1974).
- <sup>21</sup>*International Tables for Crystallography*, edited by T. Hahn (Kluwer Academic, Dordrecht, 1992).